Electronic supplementary information for:

Efficient symmetry breaking spin–orbit charge transfer-induced intersystem crossing in compact orthogonal perylene-phenothiazine or-phenoxazine triads and observation of the delayed fluorescence

Muhammad Imran,[a,§] Junhong Pang,[b,§] Jianzhang Zhao[a,c]* and Ming-De Li[b,]*

[a]State Key Laboratory of Fine Chemicals, School of Chemical Engineering, Dalian University of Technology, 2 Ling Gong Rd., Dalian 116024, P. R. China.
E-mail: zhaojzh@dlut.edu.cn

[b]Department of Chemistry and Key Laboratory for Preparation and Application of Ordered Structure Materials of Guangdong Province, Shantou University, Shantou 515063, P. R. China. E-mail: mdli@stu.edu.cn

[c]State Key Laboratory of Chemistry and Utilization of Carbon Based Energy Resources, College of Chemistry, Xinjiang University, Urumqi 830017, P. R. China.

§ These authors contributed equally to this work.

Contents

1. General information

All the chemicals were analytically pure and used as received throughout the synthesis. ^{1}H and ^{13}C NMR shifts are reported in parts per millions (ppm) relative to TMS, with the residual peaks are used as internal reference. The mass spectra were measured by TOF-HRMS-MALDI and TOF-MS-EI spectrometers.

2. Synthesis and characterization data

Synthesis of Pery-2Br.[1] In a 500 mL double-neck round bottom flask, perylene (2.0 g, 7.92 mmol) was dissolved in dry THF (320 mL). To this solution, *N*-bromosuccinimide (NBS) (4.24 g, 23.8 mmol) was added in one portion. The reaction mixture was stirred overnight at RT. After 30 h, the mixture was slowly poured into water (1500 mL) and stirred for 30 minutes. The solid dibromoperylene was collected by filtration and dried under vacuum. A yellow solid was obtained (2.4 g, yield 91%). By following the literature method,[2] 3,9-dibromoperylene was obtained after repeated recrystallization from aniline/nitrobenzene (1:1) 10 mL/10 mL mixture solution on heating at 160 °C. The ratio of regio-isomer (3,9-dibromoperylene) was checked on the basis of ^{1}H-NMR spectra. The 3,9-dibromoperylene regio-isomer was obtained with a ratio of 71 to 29 with 3,10-dibromoperylene and used for the next reactions. Mp: > 250 °C. ^{1}H NMR ($CDCl_3$, 400 MHz): δ = 8.20 (d, 2H, J = 8.0 Hz), 8.11 (d, 2H, J = 12.0 Hz), 7.95 (dd, 2H, J_1 = 8.0 Hz, J_2 = 8.0 Hz), 7.77 – 7.72 (m, 2H), 7.60 – 7.54 (m, 2H). TOF MS EI^{+}: Calcd ($[C_{20}H_{10}Br_2]^{+}$), m/z = 407.9149; found, m/z = 407.9160.

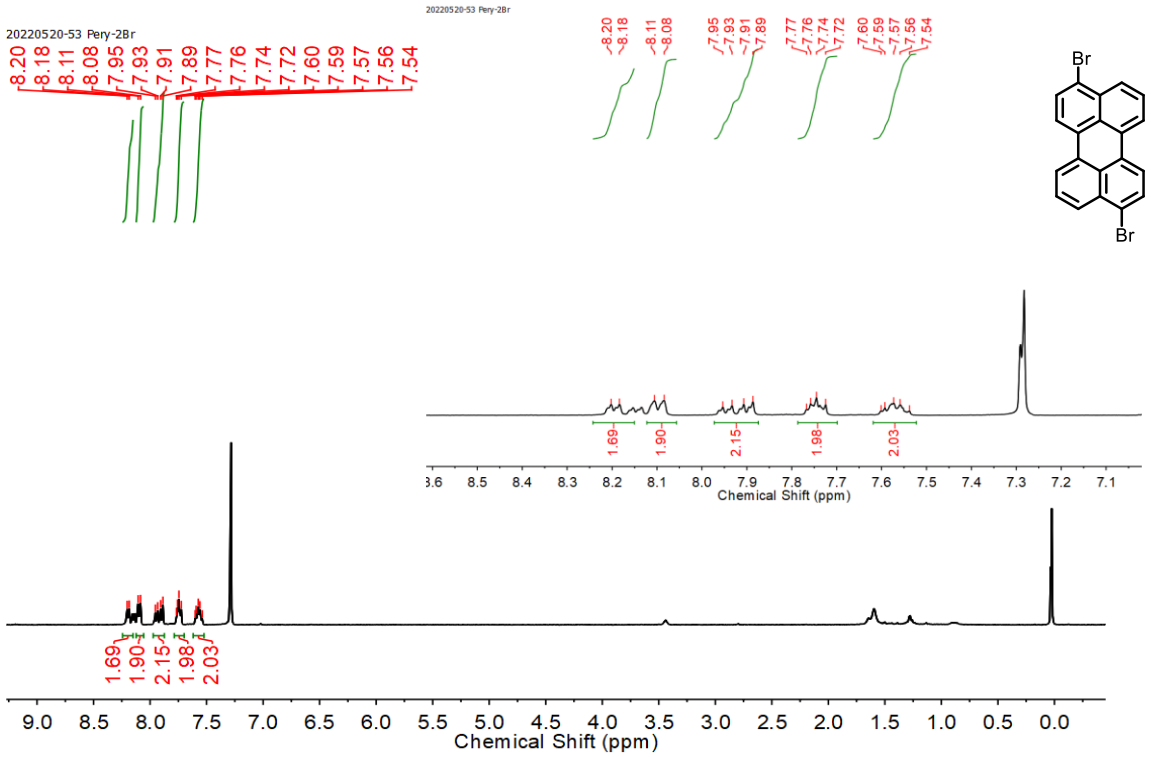

Fig. S1 ^{1}H NMR spectrum of **Pery-2Br** ($CDCl_3$, 400 MHz).

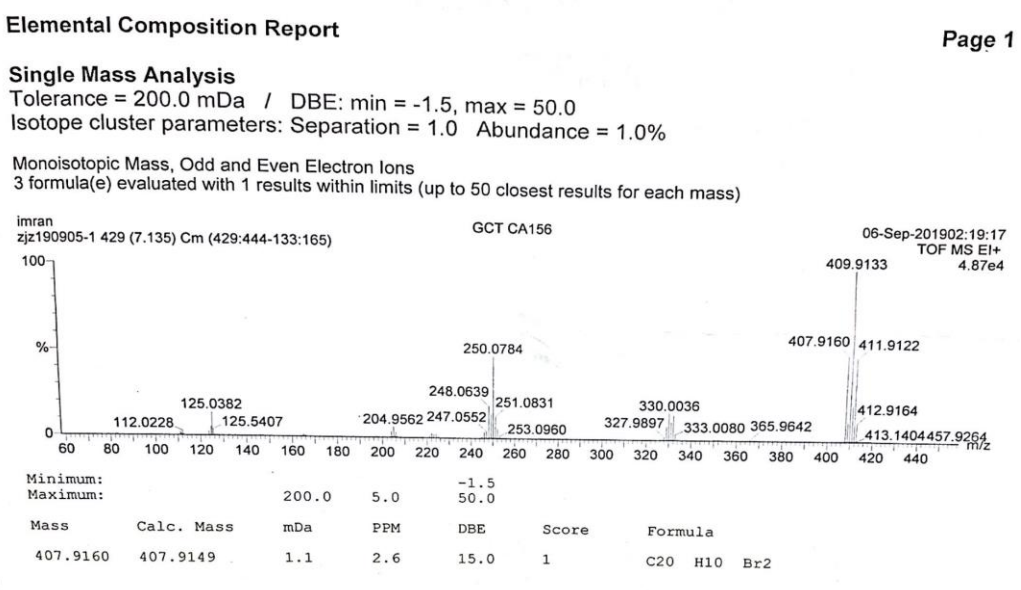

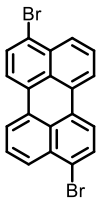

Fig. S2 TOF-MS EI^{+} spectrum of **Pery-2Br**.

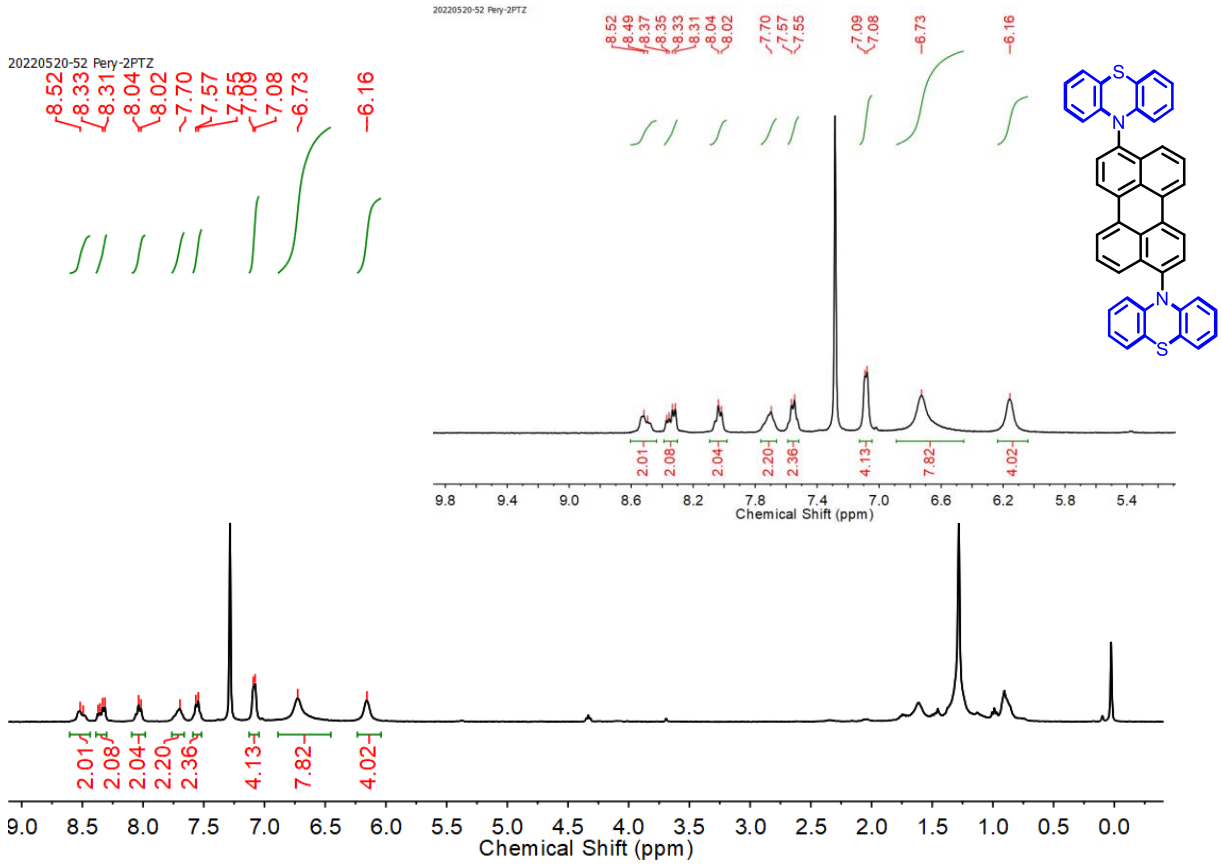

Fig. S3 ^{1}H NMR spectra of **Pery-2PTZ** ($CDCl_3$, 400 MHz).

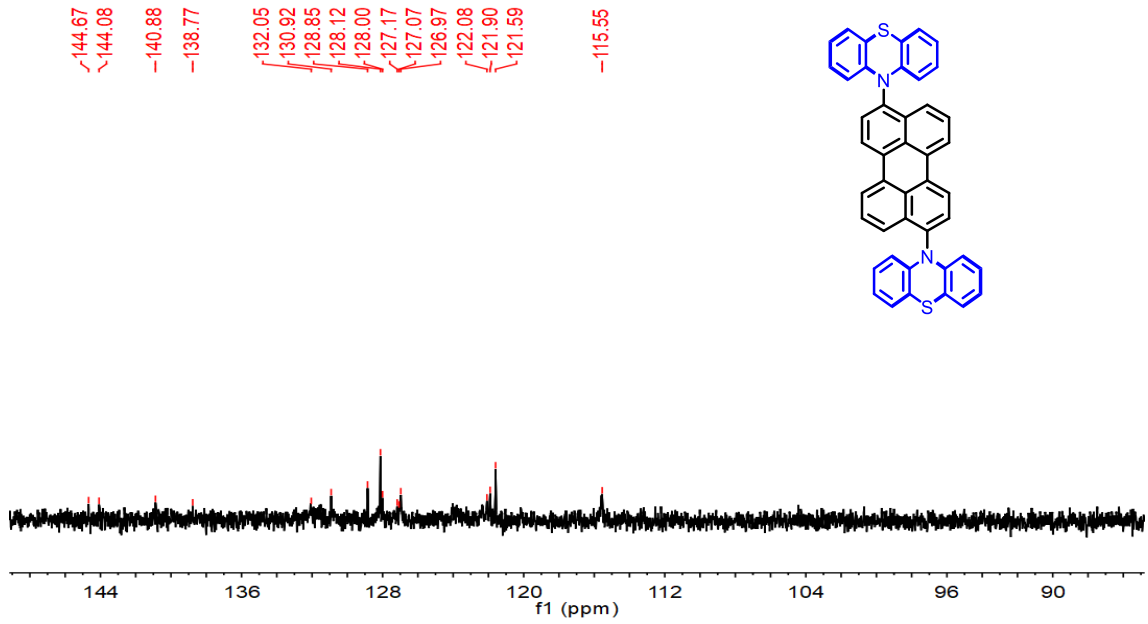

Fig. S4 ^{13}C NMR spectrum of **Pery-2PTZ** ($CDCl_3$, 126 MHz).

Smart Formula

Formula	Mass	Error	mSigma	DblEq	N rule	Electron Configuration
$C_{44}H_{26}N_2S_2$	646.1532	2.6206	34.0388	33.00	ok	odd

M$^{+\cdot}$

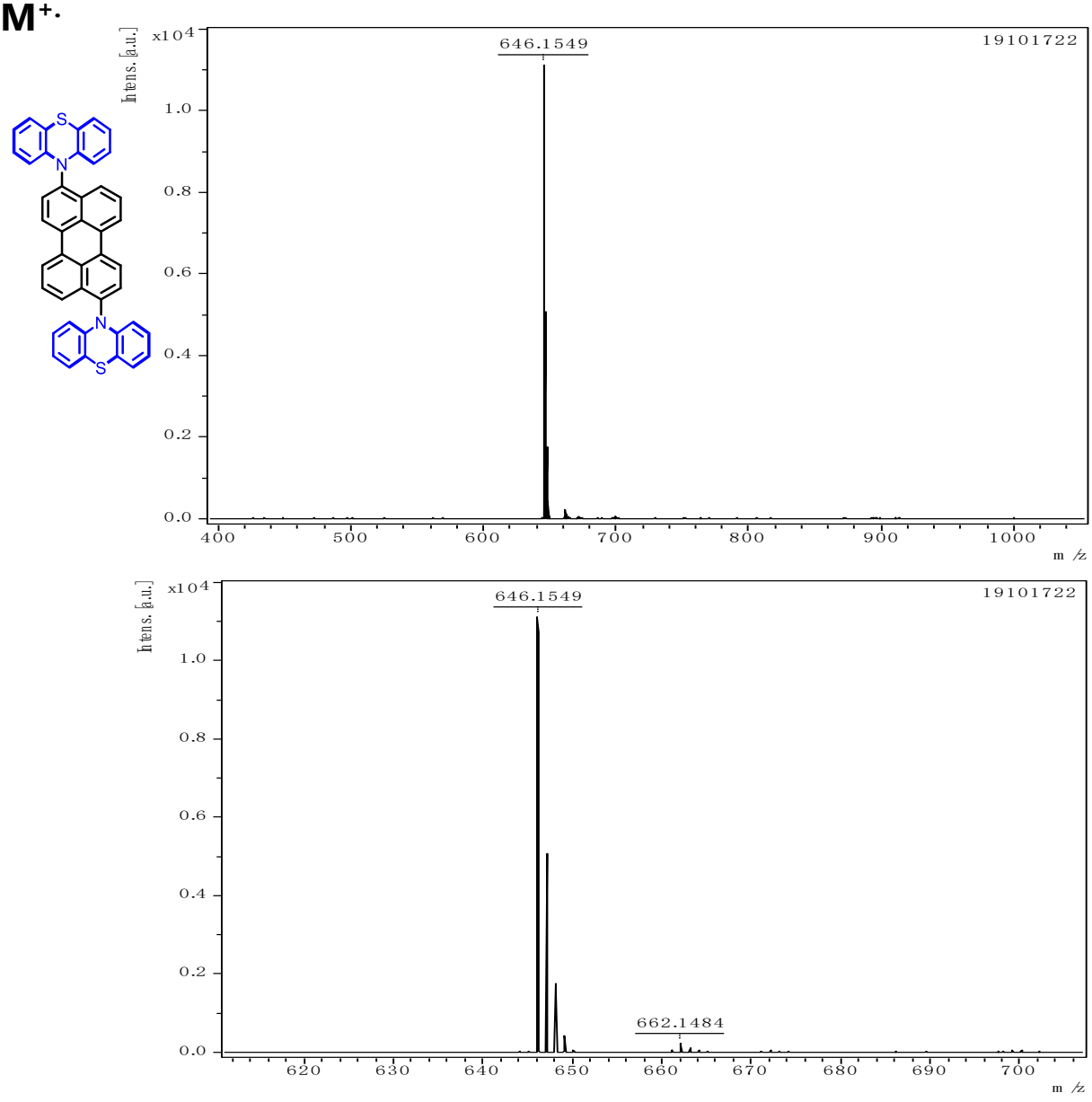

Fig. S5 MALDI-HRMS of **Pery-2PTZ.**

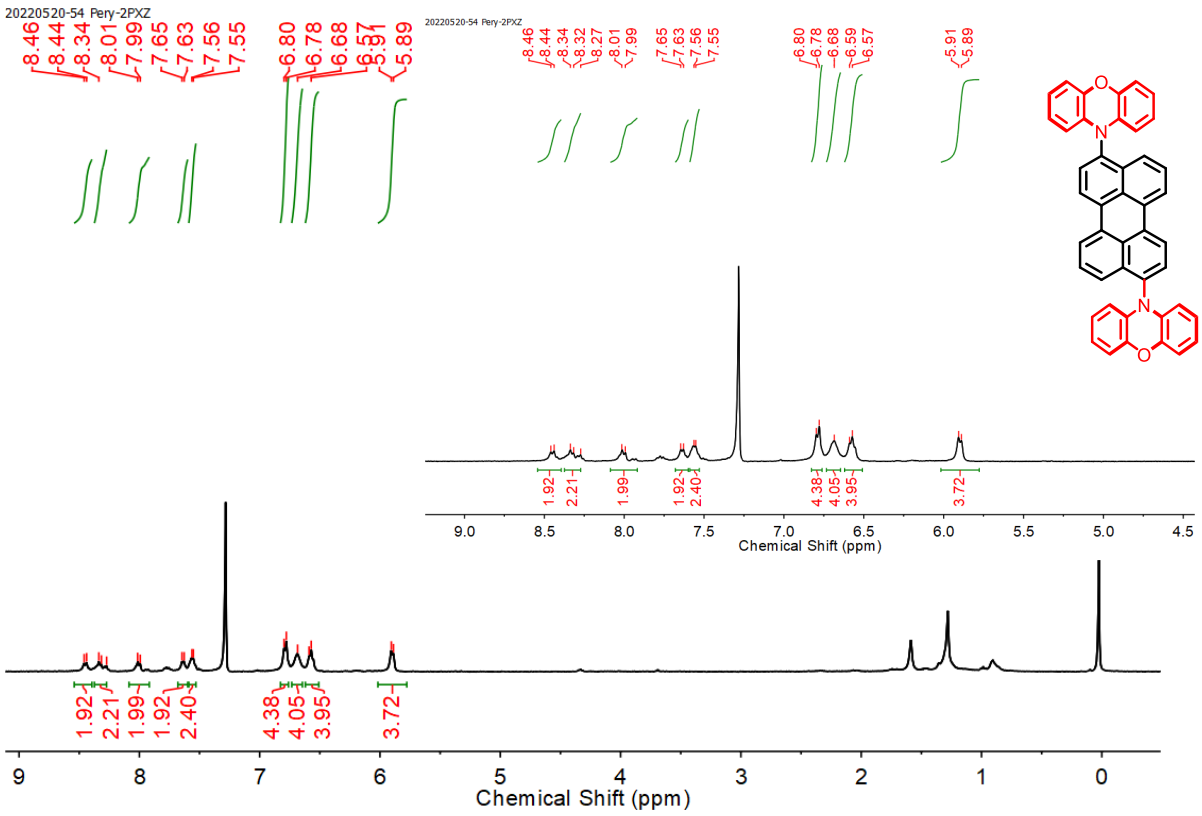

Fig. S6. ^{1}H NMR spectra of **Pery-2PXZ** ($CDCl_3$, 400 MHz).

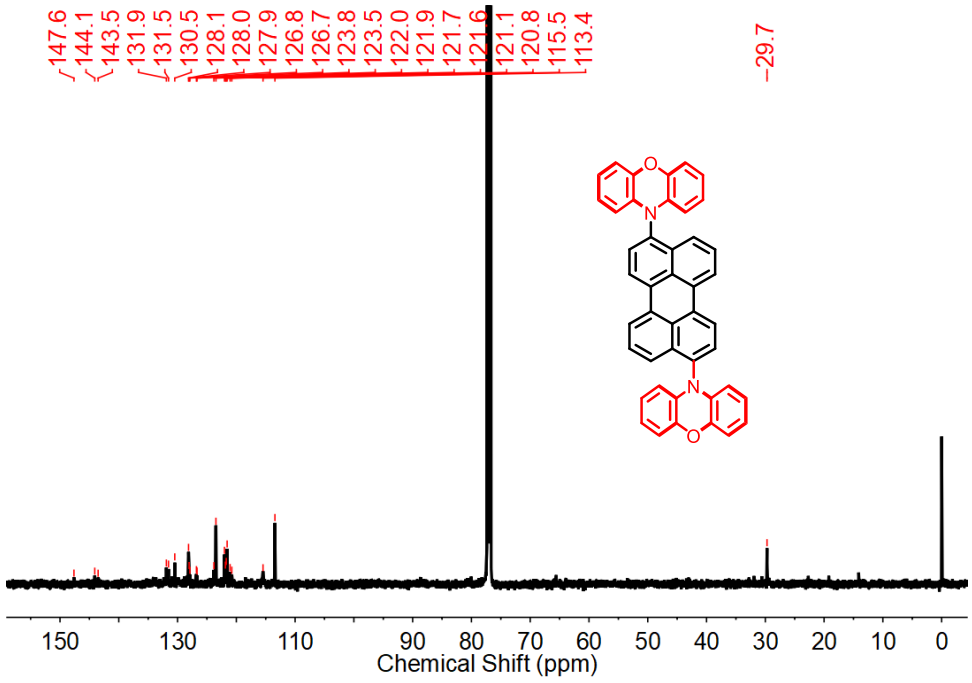

Fig. S7 ^{13}C NMR spectrum of **Pery-2PXZ** ($CDCl_3$, 126 MHz).

Smart Formula

Formula	Mass	Error	mSigma	DblEq	N rule	Electron Configuration
C_{44} H_{26} N_2 O_2	614.1994	0.6970	38.6447	33.00	ok	odd

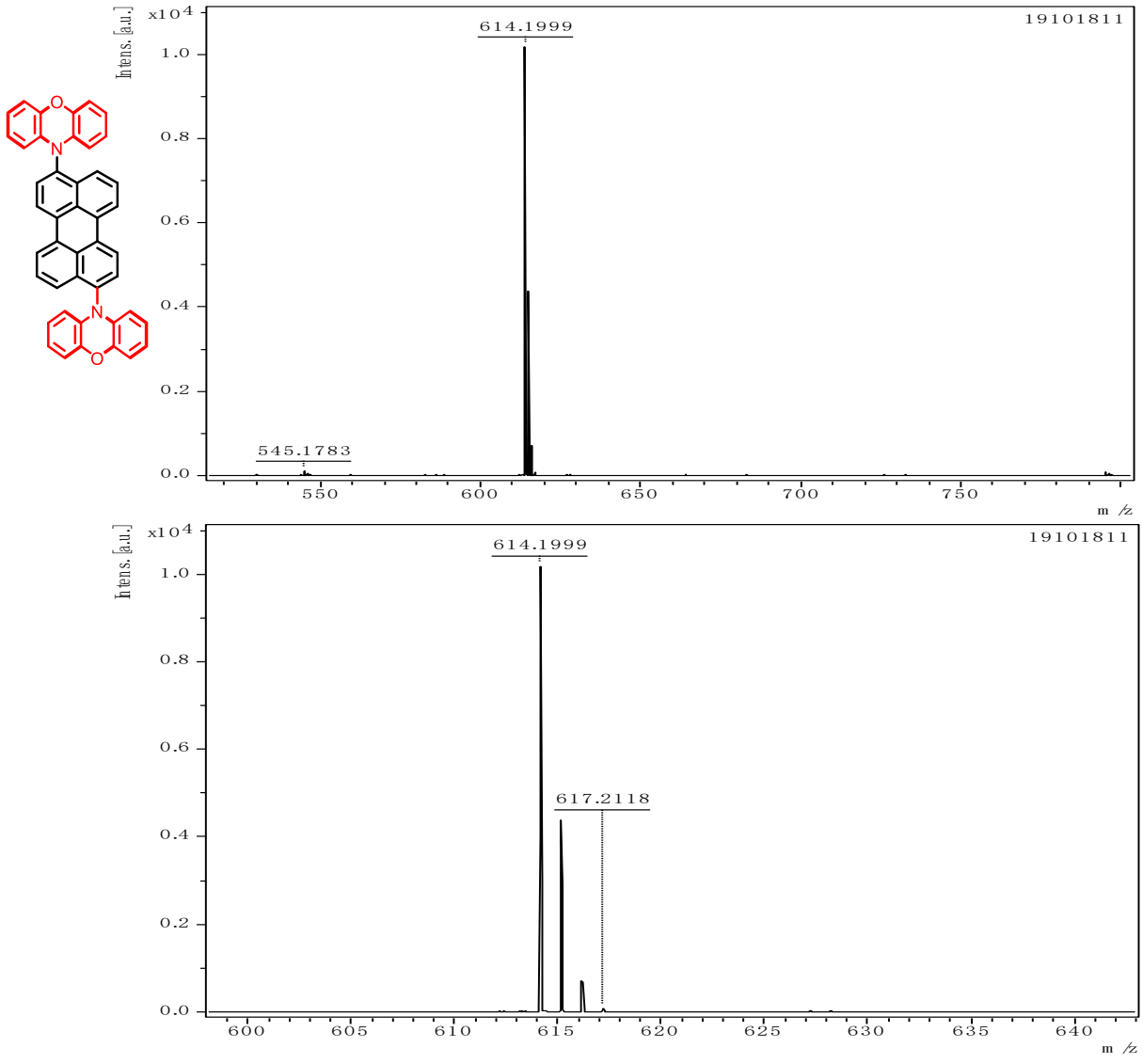

Fig. S8 MALDI-HRMS of **Pery-2PXZ.**

3. UV–vis absorption spectra

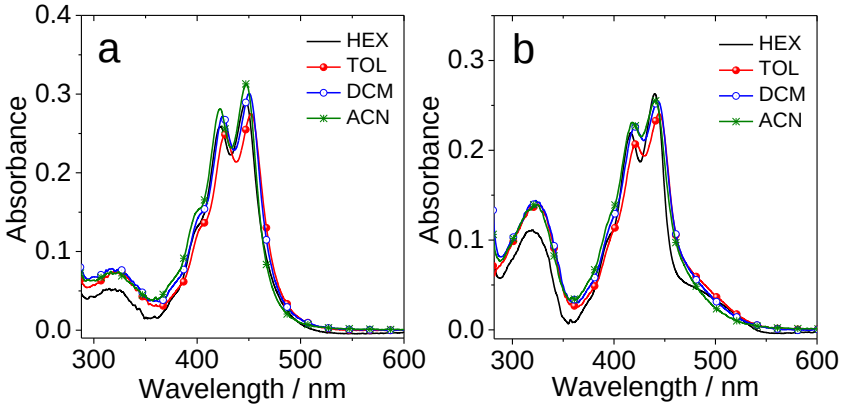

Fig. S9 UV−vis absorption spectra of the compounds in different solvents, (a) **Pery-2PTZ** (b) **Pery-2PXZ**. c = 1.0 × 10^{-5} M, 20 °C.

4. Fluorescence emission spectra and decay traces

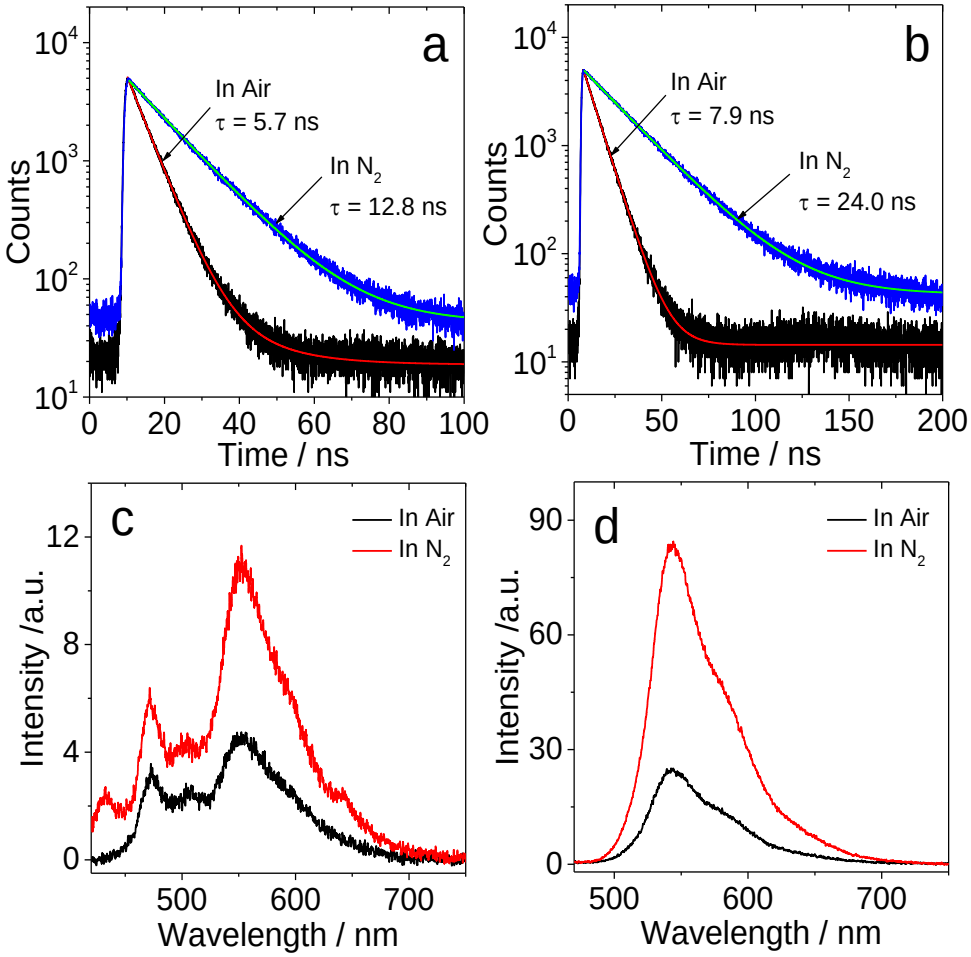

Fig. S10 Fluorescence decay traces of (a) **Pery-2PTZ** at 551 nm; (b) **Pery-2PXZ** at 544 nm, (λ_{ex} = 445 nm) and Fluorescence emission spectra of (c) **Pery-2PTZ**, (d) **Pery-2PXZ**, (λ_{ex} = 400 nm) under different atmospheres (air and N_2). *c* = ca. 1.0 × 10^{-5} M, in *n*-hexane. 20 °C.

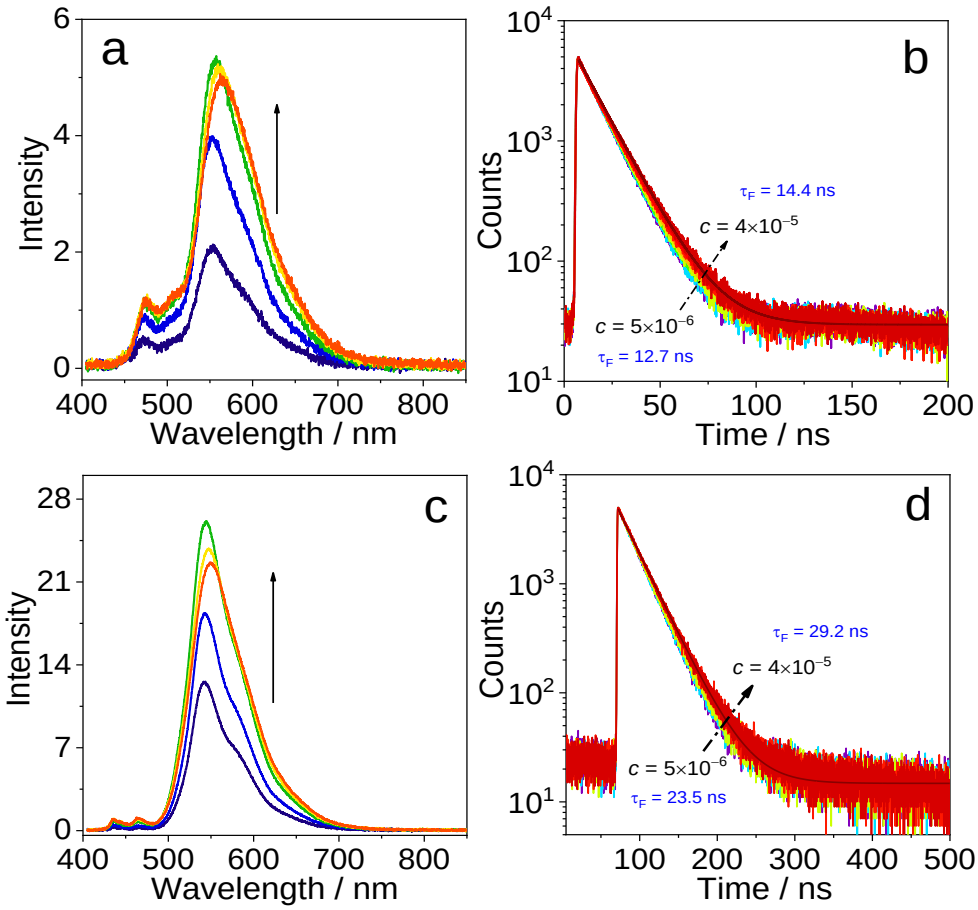

Fig. S11 Concentration-dependent fluorescence emission spectra and emission lifetime decay traces under N_2 atmosphere with increasing concentration (from $c = 5.0 \times 10^{-6}$ M to $c = 4.0 \times 10^{-5}$ M) of (a, b) **Pery-2PXZ** and (c, d) **Pery-2PXZ**, λ_{ex} = 400 nm for emission and λ_{ex} = 445 nm for lifetime decay trace. In *n*-hexane. 20 °C.

5. Electrochemical study

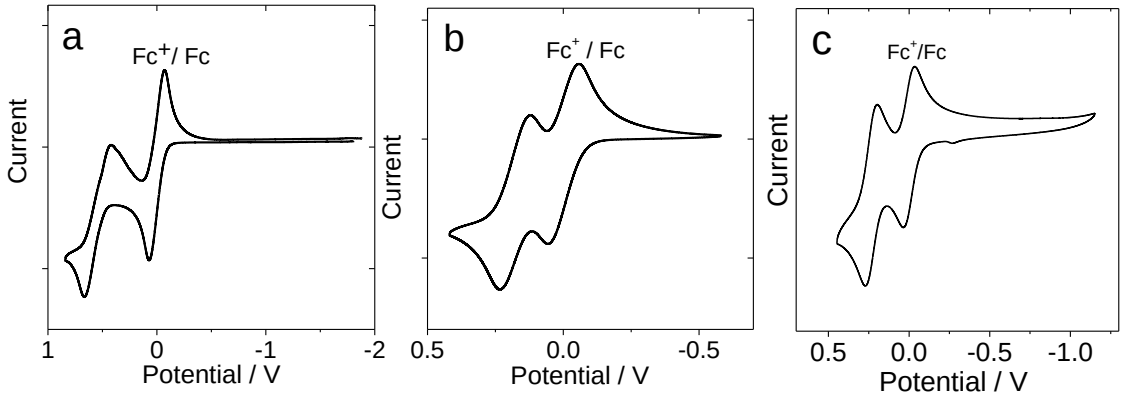

Fig. S12 Cyclic voltammogram of the compounds (a) perylene, (b) phenothiazine and (c) phenoxazine. Ferrocene was used as an internal reference. Condition: in deaerated DCM containing 0.10 M $Bu_4N[PF_6]$ as supporting electrolyte, $Ag/AgNO_3$ as the reference electrode. Scan rates: 50 mV/s. c = 1.0 × 10^{-3} M. 20 °C.

$$\Delta G^{0}_{\mathrm{CS}} = e[E_{OX} - E_{RED}] - E_{00} + \Delta G_{\mathrm{S}} \qquad \text{(Eq. S1)}$$

$$\Delta G_{\mathrm{S}} = -\frac{e^2}{4\pi\varepsilon_{\mathrm{s}}\varepsilon_0 R_{CC}} - \frac{e^2}{8\pi\varepsilon_0}\left(\frac{1}{R_{\mathrm{D}}} + \frac{1}{R_{\mathrm{A}}}\right)\left(\frac{1}{\varepsilon_{REF}} - \frac{1}{\varepsilon_{\mathrm{S}}}\right) \qquad \text{(Eq. S2)}$$

$$\Delta G_{\mathrm{CR}} = -\left(\Delta G_{\mathrm{CS}} + E_{00}\right) \qquad \text{(Eq. S3)}$$

$$E_{CSS} = e[E_{OX} - E_{RED}] + \Delta G_S \qquad \text{(Eq. S4)}$$

where ΔG_S is the static Coulombic energy, which is defined by eq. S2. e = electronic charge, E_{OX} = half-wave potential of the electron-donor unit for one-electron oxidation, E_{RED} = half-wave potential of the electron-acceptor unit for one-electron reduction; E_{00} =

approximated energy level with the cross point of normalized UV−Vis absorption and fluorescence emission spectra at singlet excited state, ε_S = static dielectric constant of the solvent, R_{CC} = center-to-center distance between electron donor unit (phenothiazine or phenoxazine) and the electron acceptor unit (perylene) determined by DFT optimization of the geometry, R_{CC} (**Pery-2PTZ**) = 6.780 Å, R_{CC} (**Pery-2PXZ**) = 6.355 Å, R_D, is the radius of the electron donor, R_A, is the radius of the electron acceptor, ε_{REF} is the static dielectric constant of the solvent used for the electrochemical studies, ε_0 is the permittivity of free space. Following solvents were used in the calculation of the free energy of electron transfer, *n*-hexane (ε_S = 1.88), toluene (ε_S = 2.38), chloroform (ε_S = 4.81), DCM (ε_S = 9.1) and ACN (ε_S = 37.5).

6. Chemical oxidation and steady-state ESR spectroscopy

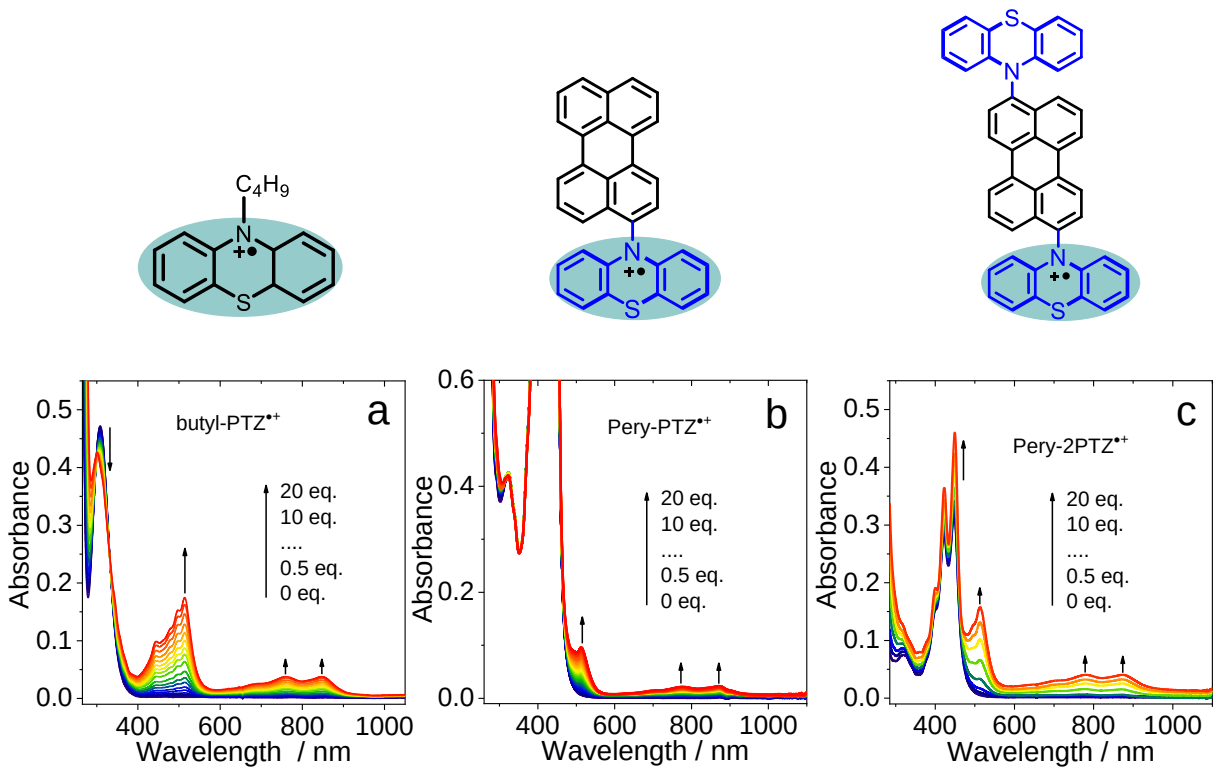

Fig. S13. Evolution of the UV−vis absorption spectra upon chemical oxidation of (a) ***n*-butyl PTZ** (b) **Pery-PTZ** and (c) **Pery-2PTZ** with nitrosonium hexafluorophosphate ($NO[PF_6]$) as an oxidant in deaerated dry ACN solvent. 20 °C.

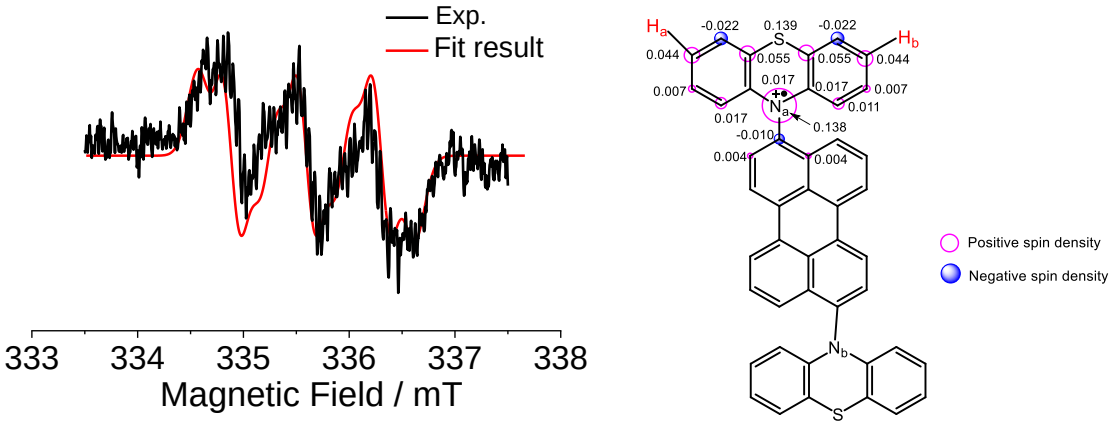

Fig. S14. (left) EPR spectra of **Pery-2PTZ**$^{\bullet+}$ in deaerated dry ACN solvent with (NO[PF_6]) as an oxidant at 300 K. c = 1.0 × 10^{-3} M. Microwave frequency = 9.41 GHz, power = 0.200 mW, and modulation amplitude = 1 G. The simulated spectrum with the best-fit hyperfine coupling constants was obtained by Easyspin. (right) Spin density of **Pery-2PTZ**$^{\bullet+}$ calculated at the B3LYP/6-31G(d) level.

Table S1. Hyperfine coupling (HFC) constants of **Pery-2PTZ**$^{\bullet+}$ and **Pery-2PXZ**$^{\bullet+}$ obtained by EPR spectral simulation and DFT calculation.

HFC (mT)		$\lvert a(N_a)\rvert$	$\lvert a(N_b)\rvert$	$\lvert a(H_a)\rvert$	$\lvert a(H_b)\rvert$	$\lvert a(H_c)\rvert$	$\lvert a(H_d)\rvert$
Pery-2PTZ	Cal.[a]	0.42	0.42	0.12	0.12		
	Exp.	0.62		0.20	0.20		
Pery-2PXZ	Cal.[a]	0.32	0.32	0.14	0.14	0.06	0.06
	Exp.	0.30		0.12	0.12	0.05	0.05

[a] HFC constants were obtained by DFT calculation of the corresponding radical cation at the B3LYP/EPR-II.

7. Singlet oxygen quantum yield determination

Singlet oxygen quantum yields of the compounds (mentioned in Table 1, in the main text) were measured with $Ru(bpy)_3[PF_6]_2$ as standard (Φ_Δ = 57% in DCM). 1,3-Diphenylisobenzofuran (DPBF) was used as the singlet oxygen ($^1O_2$) scavenger to monitor the $^1O_2$ production by following the change of absorption of DPBF at 414 nm upon photoirradiation. To determine the singlet oxygen quantum yield (Φ_Δ), eq. S5 was used.

$$\Phi_{\Delta,sam} = \Phi_{\Delta,std}\left(\frac{1-10^{-A_{std}}}{1-10^{-A_{sam}}}\right)\left(\frac{m_{sam}}{m_{std}}\right)\left(\frac{\eta_{sam}}{\eta_{std}}\right)^2 \qquad \text{(Eq. S5)}$$

Where '*sam*' and '*std*' designate the compounds and standard, respectively, *A* is the absorbance at the excitation wavelength, *m* is the slope of the plot of absorbance of DPBF at 414 nm versus the irradiation time, η is the refractive index of the solvent used for the measurements. The sample and the standard solutions should have the same absorbance at the excitation wavelength, for this purpose optically matched solutions were used.

8. Femtosecond transient absorption spectral study

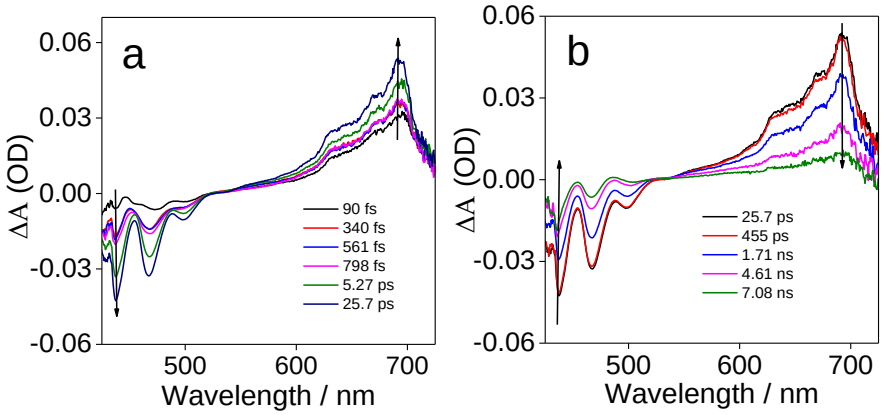

Fig. S15 Femtosecond transient absorption spectra of pristine perylene in DCM (a) at initial delays (b) at long time delays, λ_{ex} = 400 nm. 20 °C.

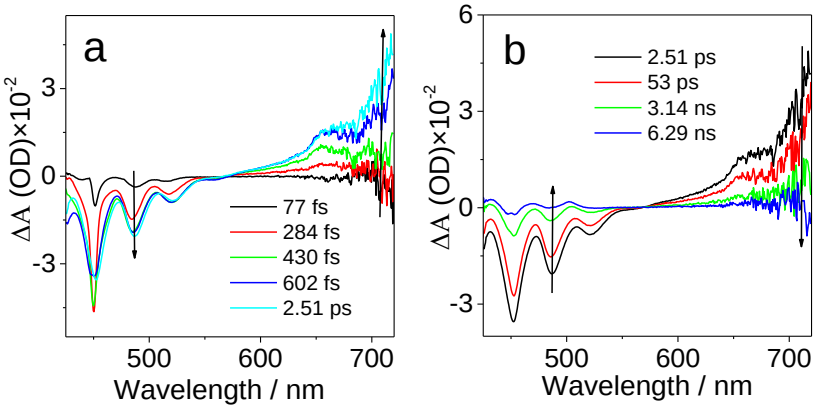

Fig. S16 Femtosecond transient absorption spectra of **Pery-2Br** in *n*-hexane (a) at initial delays (b) at long time delays, λ_{ex} = 400 nm. 20 °C.

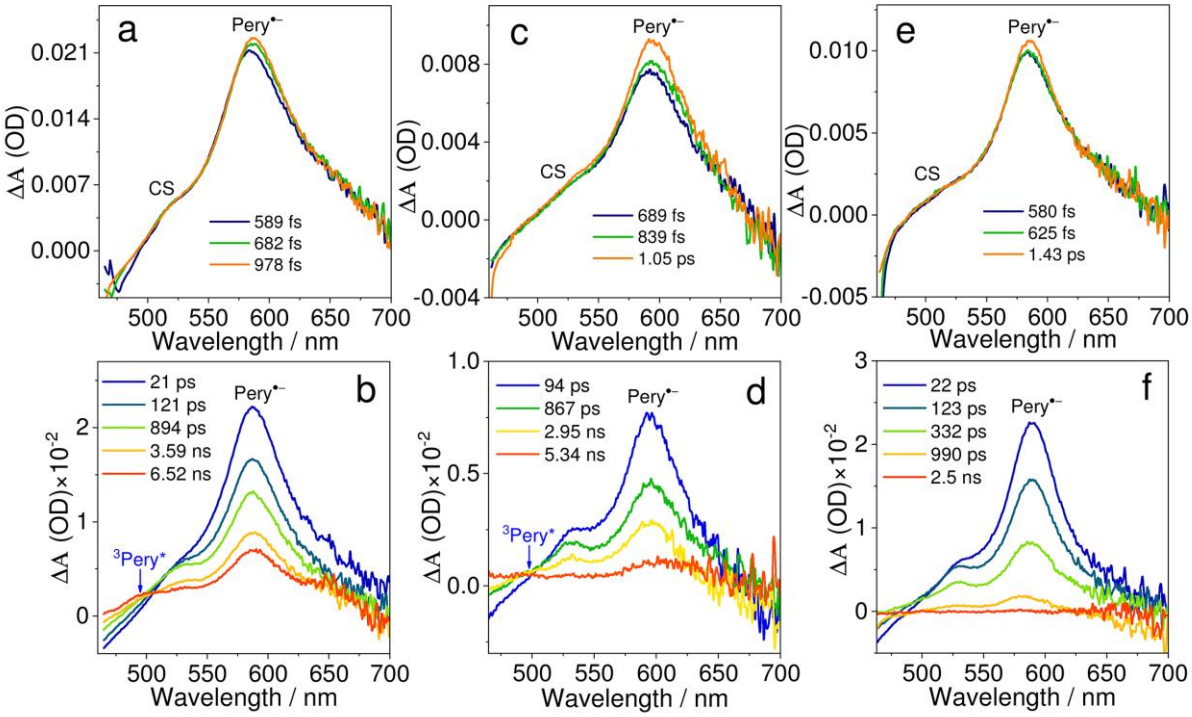

Fig. S17 Femtosecond transient absorption spectra of **Pery-2PXZ**, (a) in n-hexane at initial delays (b) in n-hexane at long time delays, (c) in DCM at initial delays (d) in DCM at long time delays and (e) in ACN at initial delays (f) in ACN at long time delays, λ_{ex} = 450 nm. 20 °C.

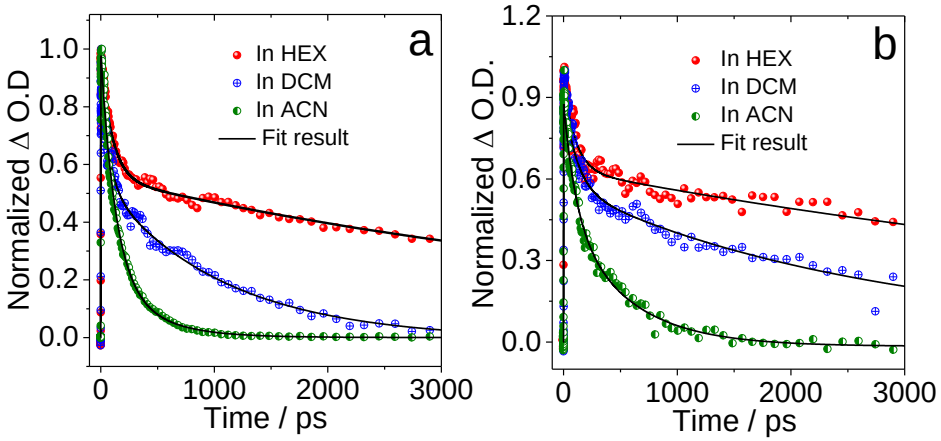

Fig. S18 The decay curves of fs-TA data in different solvents at 590 nm of (a) **Pery-2PTZ** and (b) **Pery-2PXZ**, λ_{ex} = 450 nm. 20 °C.

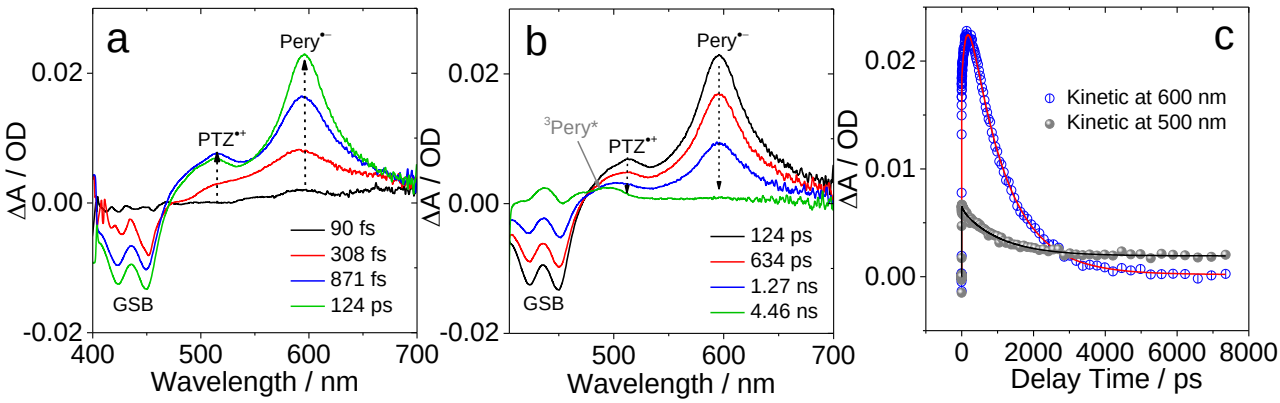

Fig. S19 Femtosecond transient absorption spectra of **Pery-2PTZ** in DCM, (a) at initial delays (b) at long time delays (c) decay traces at selected wavelengths. GSB; Ground state bleach, λ_{ex} = 400 nm. 20 °C.

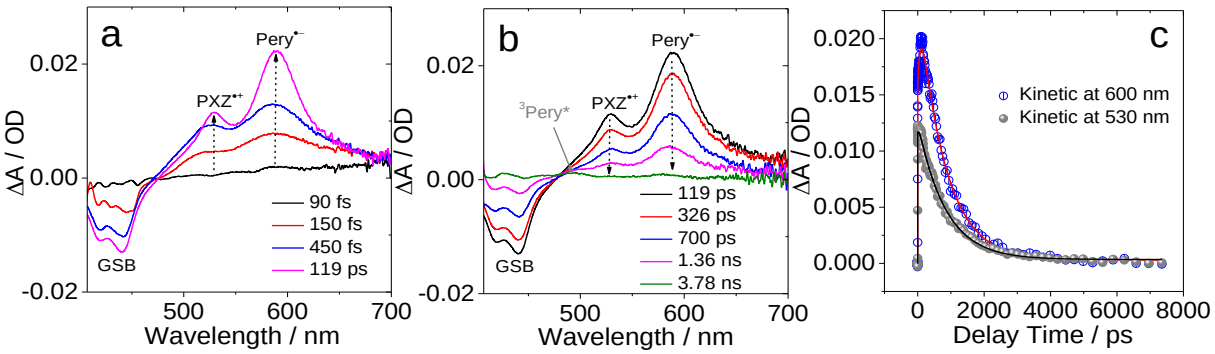

Fig. S20 Femtosecond transient absorption spectra of **Pery-2PXZ** in DCM, (a) at initial delays (b) at long time delays (c) decay traces at selected wavelengths. GSB; Ground state bleach, λ_{ex} = 400 nm. 20 °C.

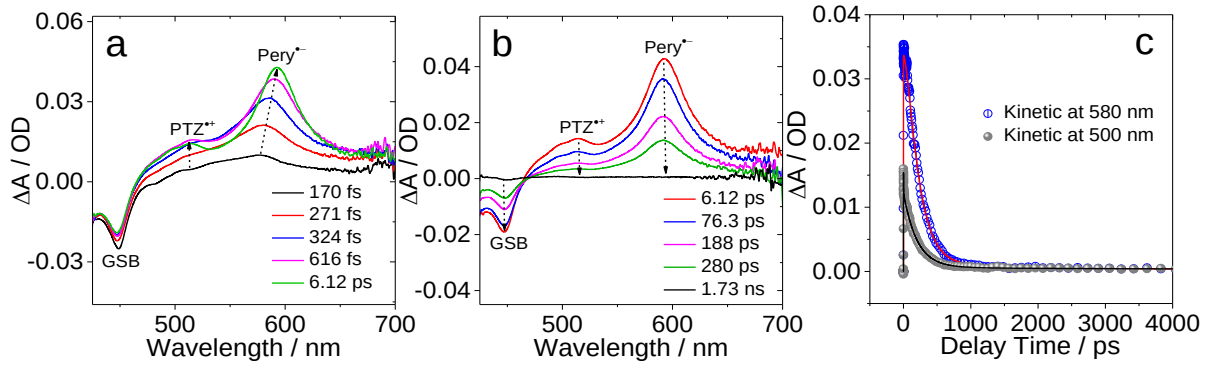

Fig. S21 Femtosecond transient absorption spectra of **Pery-2PTZ** in ACN, (a) at initial delays (b) at long time delays (c) decay traces at selected wavelengths. GSB; Ground state bleach, λ_{ex} = 400 nm. 20 °C.

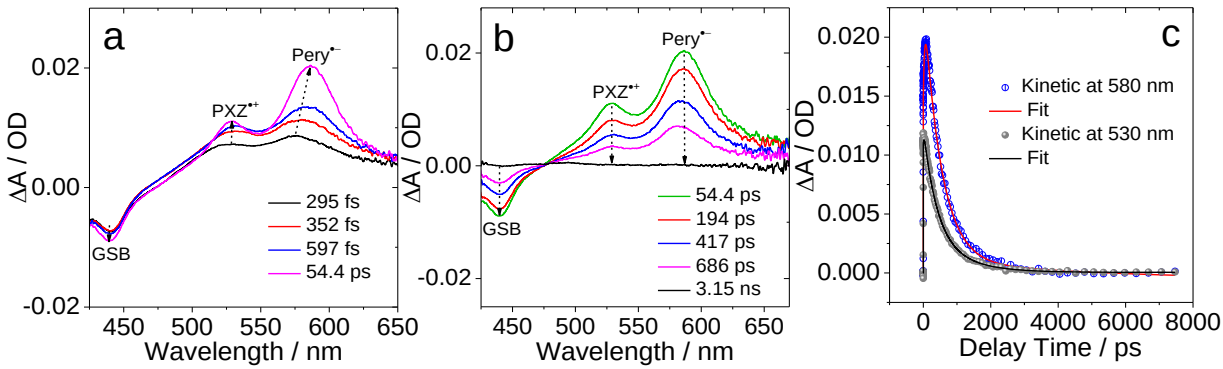

Fig. S22 Femtosecond transient absorption spectra of **Pery-2PXZ** in ACN, (a) at initial delays (b) at long time delays (c) decay traces at selected wavelengths. GSB; Ground state bleach, λ_{ex} = 400 nm. 20 °C.

9. Nanosecond transient absorption spectroscopy

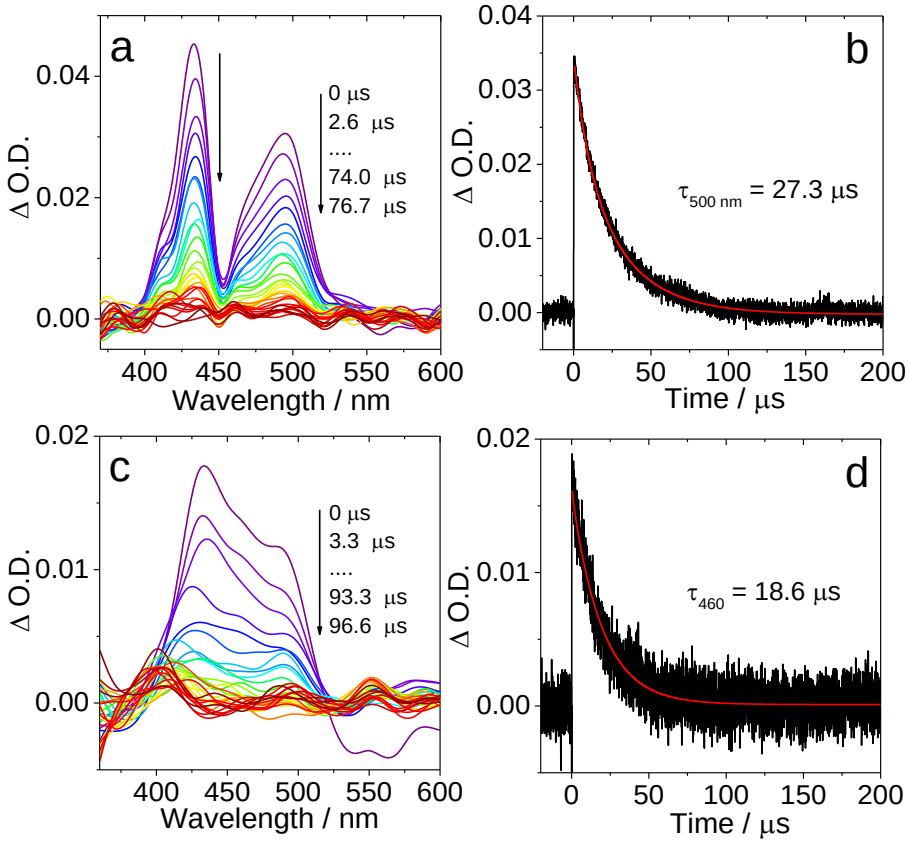

Fig. S23 Nanosecond transient absorption spectra of (a) **Pery-2PTZ**, (b) decay trace at 500 nm; (c) **Pery-2PXZ** and (d) decay trace at 450 nm. c = 2.0 × 10^{-5} M. In deaerated *n*-hexane, λ_{ex} = 460 nm. 20 °C.

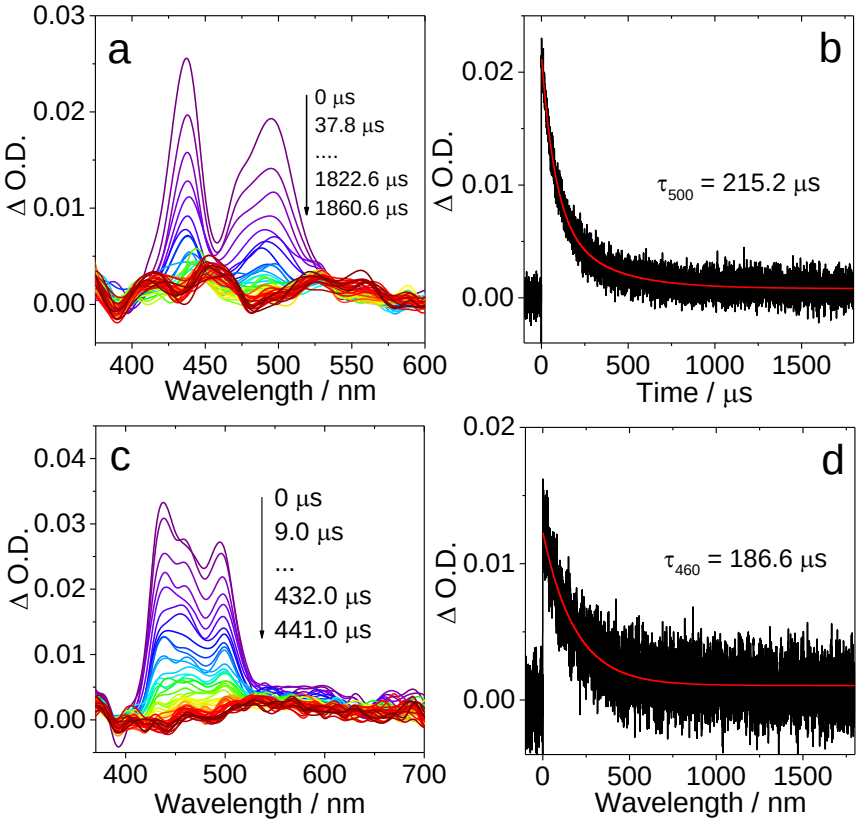

Fig. S24 Nanosecond transient absorption spectra of (a) **Pery-2PTZ**, (b) decay trace at 500 nm; (c) **Pery-2PXZ**, and (d) decay trace at 450 nm. c = 2.0 × 10^{-5} M. In deaerated $CHCl_3$, λ_{ex} = 460 nm. 20 °C.

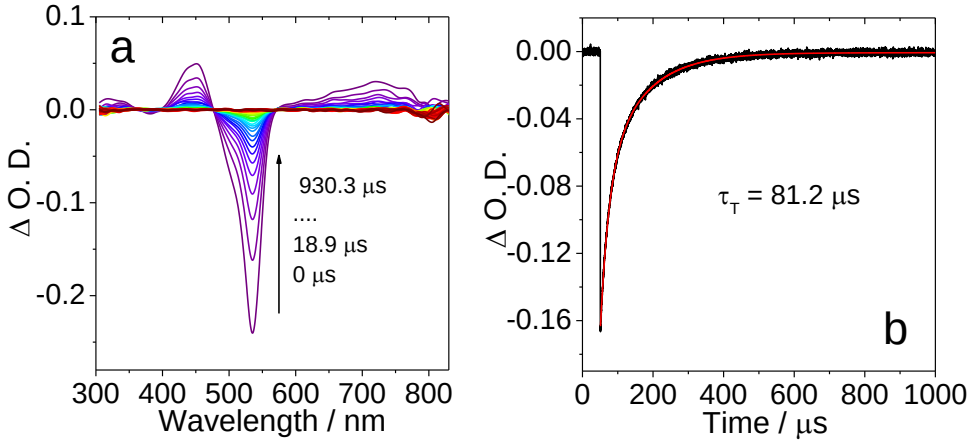

Fig. 25 (a) Nanosecond transient absorption spectra of **diiodo-BDP** and (b) decay trace at 520 nm; *c* (**diiodo-BDP**) = 1.0 × 10^{-5} M, in deaerated ACN, λ_{ex} = 532 nm. 20 °C.

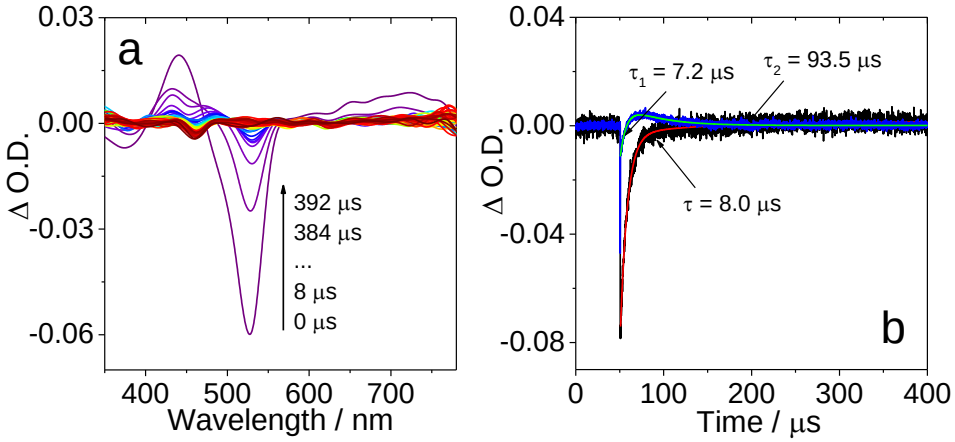

Fig. S26 Intermolecular TTET with **diiodo-BDP** as triplet energy donor and **Pery-2PXZ** as energy acceptor: (a) ns-TA spectra of the mixture of **diiodo-BDP** (*c* = 2.0 × 10^{-5} M) and **Pery-2PXZ** (*c* = 1.0 × 10^{-5} M) and (b) decay trace at 490 nm, showing the rise and decay phases of TTET process. In deaerated *n*-hexane, λ_{ex} = 532 nm. 20 °C.

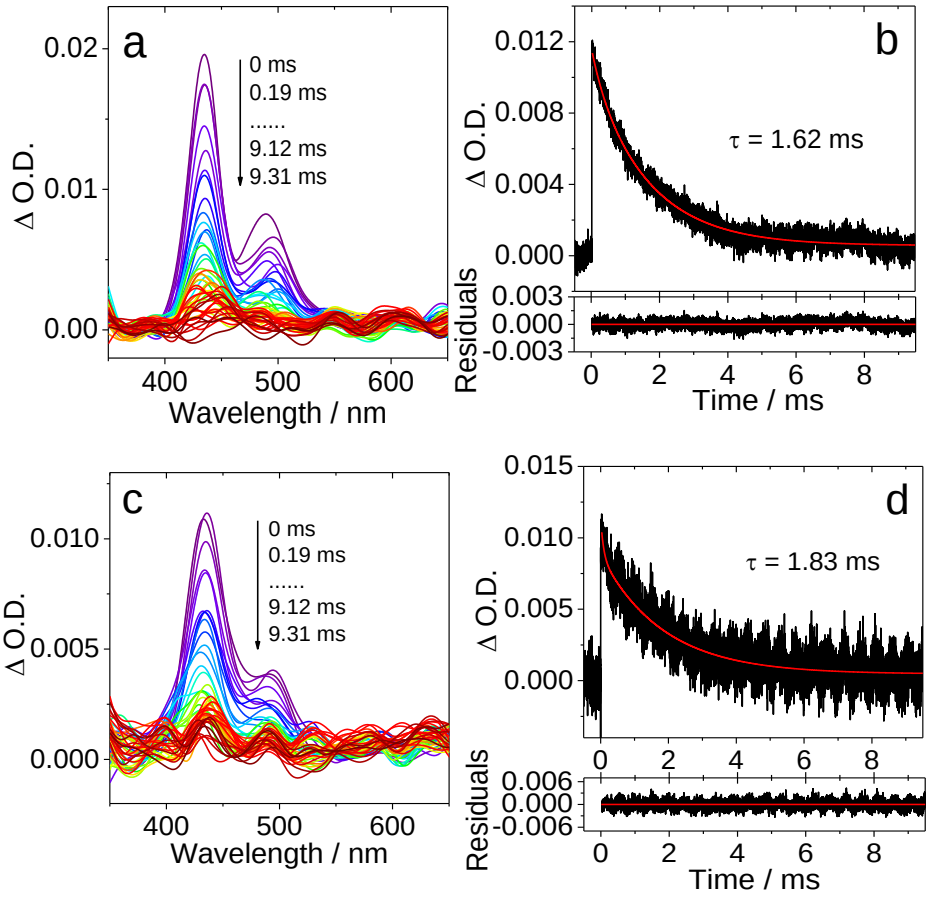

Fig. S27 Nanosecond transient absorption spectra of (a) **Pery-2PTZ,** (b) decay trace at 490 nm, (c) **Pery-2PXZ** and (d) decay trace at 450 nm. In deaerated glycerol triacetate. *c* = 2.0 × 10^{-5} M, λ_{ex} = 445 nm, 20 °C.

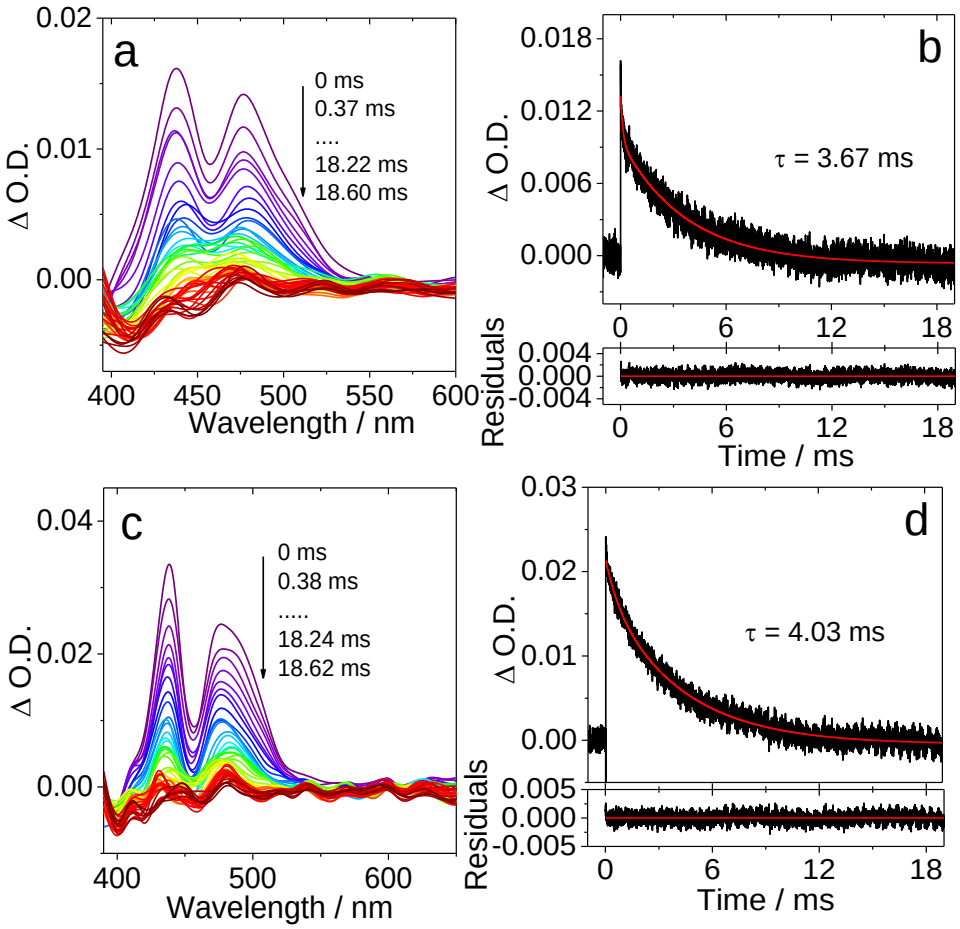

Fig. S28 Nanosecond transient absorption spectra of **Pery-2PTZ** in Clear Flex 50 polymer film (a and b) under deaerated conditions and (c and d) under aerated conditions. Decay traces are taken at 490 nm in both cases, λ_{ex} = 445 nm. 20 °C.

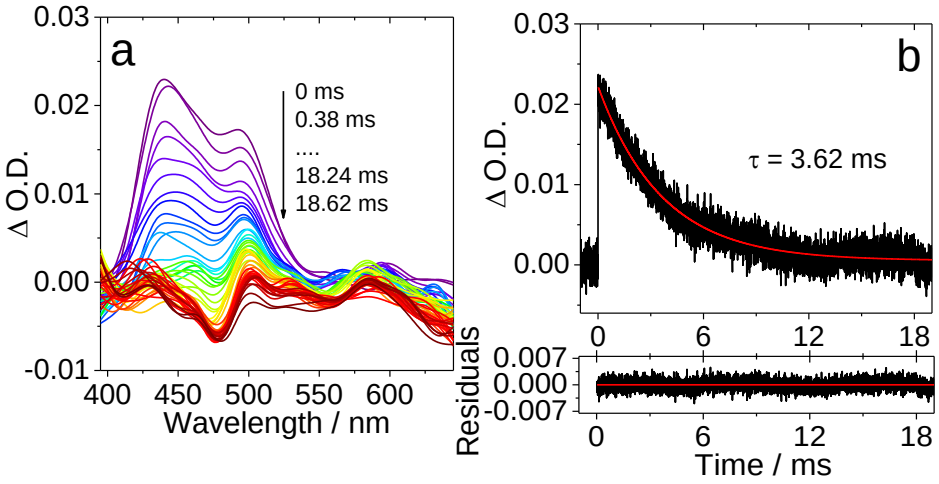

Fig. S29 (a) Nanosecond transient absorption spectra of **Pery-2PXZ** in Clear Flex 50 film under deaerated condition and (b) decay trace at 490 nm, λ_{ex} = 440 nm. 20 °C.

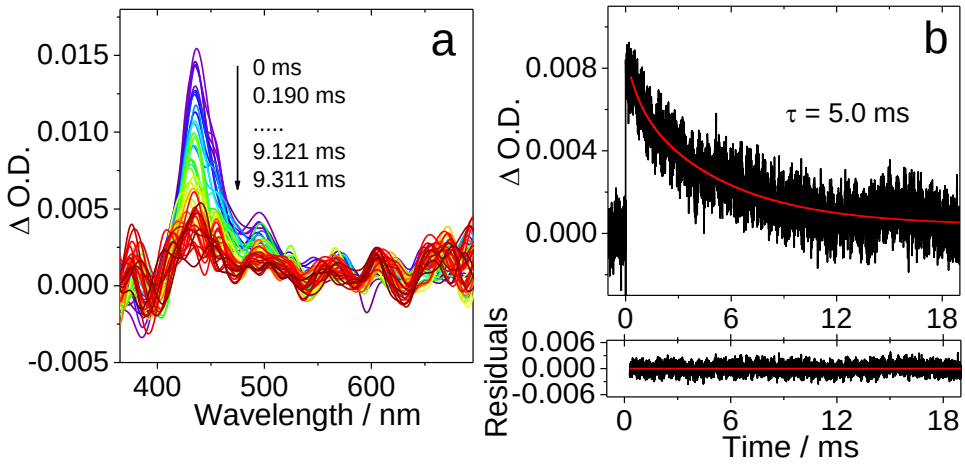

Fig. S30 (a) Nanosecond transient absorption spectra of **Pery-2PXZ** in polymethylmethacrylate (PMMA) dopped film under deaerated condition and (b) decay trace at 455 nm, λ_{ex} = 440 nm. 20 °C.

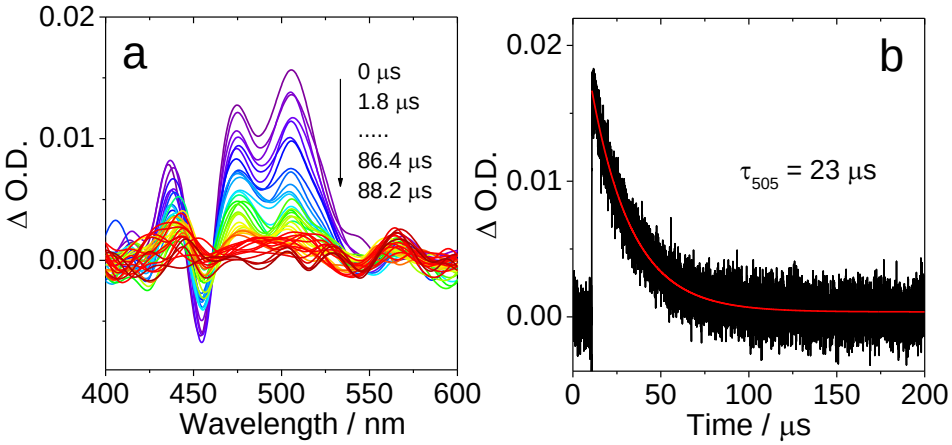

Fig. S31 (a) Nanosecond transient absorption spectra of **Pery-2Br** and (b) decay trace at 505 nm, λ_{ex} = 440 nm. c = 2.0 × 10^{-5} M. In deaerated toluene. 20 °C.

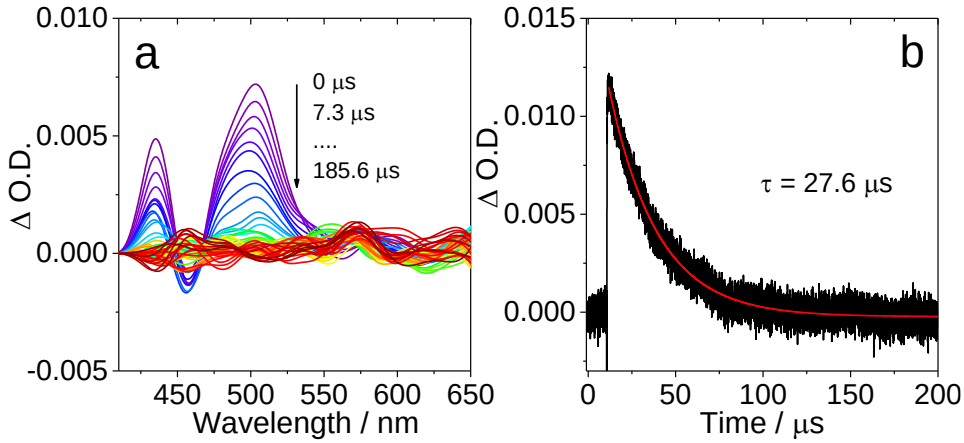

Fig. S32 (a) Nanosecond transient absorption spectra of **Pery-2Br** in film (Clear Flex 50) and (b) decay trace at 505 nm, λ_{ex} = 440 nm. 20 °C.

10. Intrinsic triplet state lifetime fitting parameters

When the intrinsic lifetime of triplet states is long and the concentration of the triplet states is high, the triplet-triplet annihilation will contribute an additional lifetime quenching factor to the decay of the transient absorption. Then triplet state lifetime will be quenched significantly and the experimental values will be shorter than the intrinsic lifetime. The corresponding differential equations for the triplet concentration fitting of the decay traces are given below. We fitted the decay curves taken at different concentrations (c = 5.0 × 10^{-6} M and 2.0 × 10^{-5} M) with a kinetic model to eliminate the TTA self-quenching effect with Eq. S6.

has the solution:

$$\frac{dc_{\mathrm{T}}}{dt} = -k_1 c_{\mathrm{T}} - k_2 {c_{\mathrm{T}}}^2 \qquad \text{(Eq. S6)}$$

$$c_{\mathrm{T}}(t) = \frac{c_0\, k_1}{\exp(k_1 t) \cdot (c_0 k_2 + k_1) - c_0 k_2} \qquad \text{(Eq. S7)}$$

Where c_0 is the initial triplet concentration. This leads to the following expression for the triplet absorption

$$A(t) = \frac{A_0 \tau_2/\tau_1}{\exp(t/\tau_1) \cdot (1 + \tau_2/\tau_1) - 1} \qquad \text{(Eq. S8)}$$

Where $A(t)$ and A_0 are the optical density (Δ O.D.) values of the triplet state decay traces at t and 0 moment; $\tau_1 = 1/k_1$ is the intrinsic triplet state lifetime; $\tau_2 = 1/c_0 k_2$ is the triplet state lifetime related with TTA quenching effect. We fitted the data sets of **Pery-2PTZ** and **Pery-2PXZ** triads triplet state lifetimes values measured in solutions simultaneously by using Eq. S8, with the variation of these parameters (A_0, τ_1, τ_2), but with the intrinsic triplet lifetime constrained to the same value in all data sets.

11. Nanosecond transient emission spectroscopy

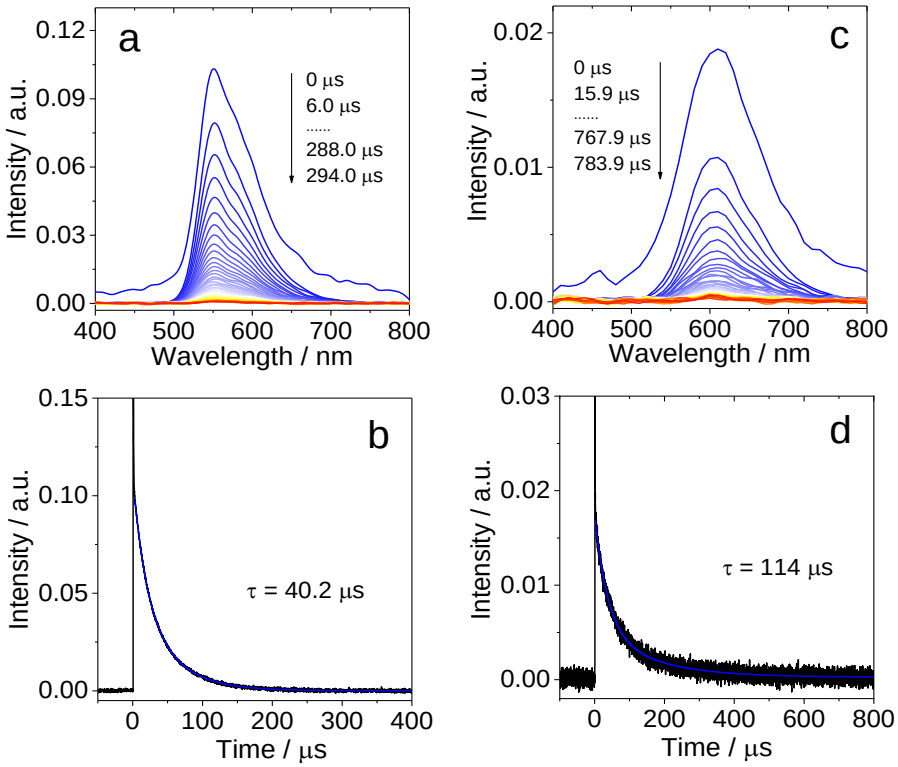

Fig. S33 Nanosecond transient emission spectra of **Pery-2PXZ** (a) in deaerated *n*-hexane, (b) respective decay trace at 550 nm, (c) in deaerated toluene and (d) respective decay trace at 610 nm. Upon pulsed laser excitation, λ_{ex} = 445 nm, 1.8 mJ/pulse, pulse duration 5 ns. c = 1.0 × 10^{-5} M. 20 °C.

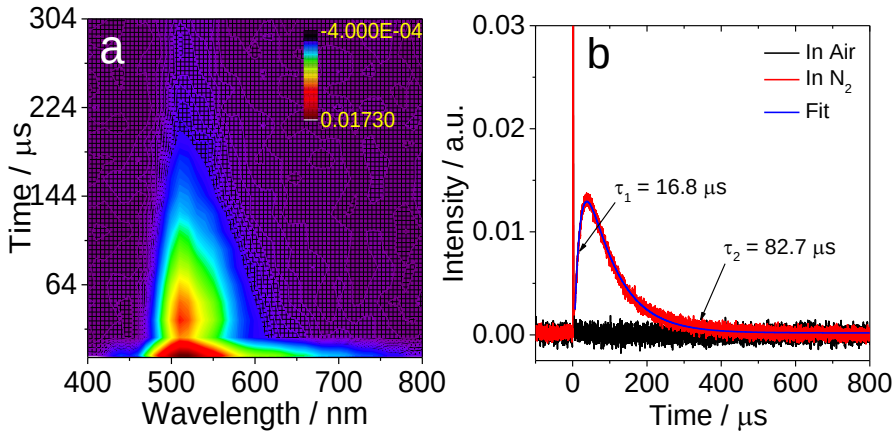

Fig. S34. (a) Delayed fluorescence 2D contour map of **Pery-2PXZ** (λ_{em} = 470 nm) and (b) Respective fluorescence decay trace at 510 nm in deaerated and aerated solutions. The spike at time 0 in (b), is the scattered laser. c = [**Pery-2PXZ**] = 1.0 × 10^{-5} M and [**SG-5**] = 2.0 × 10^{-5} M. In deaerated $CHCl_3$, λ_{ex} = 445. 20 °C.

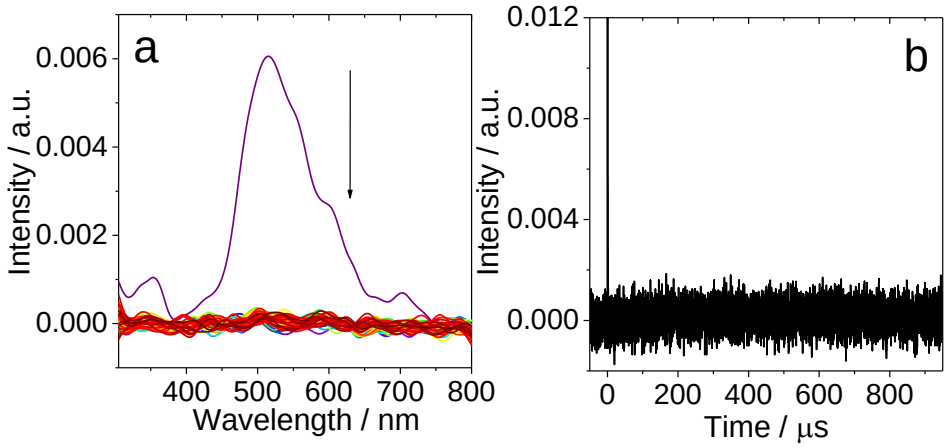

Fig. S35. (a) Delayed fluorescence of **Pery-2PXZ** in deaerated glycerol triacetate, (b) Respective fluorescence decay trace at 510 nm. c = [**Pery-2PXZ**] = 1.0 × 10^{-5} M and [**SG-5**] = 2.0 × 10^{-5} M, λ_{ex} = 445. 20 °C.

12. Density functional theory calculations

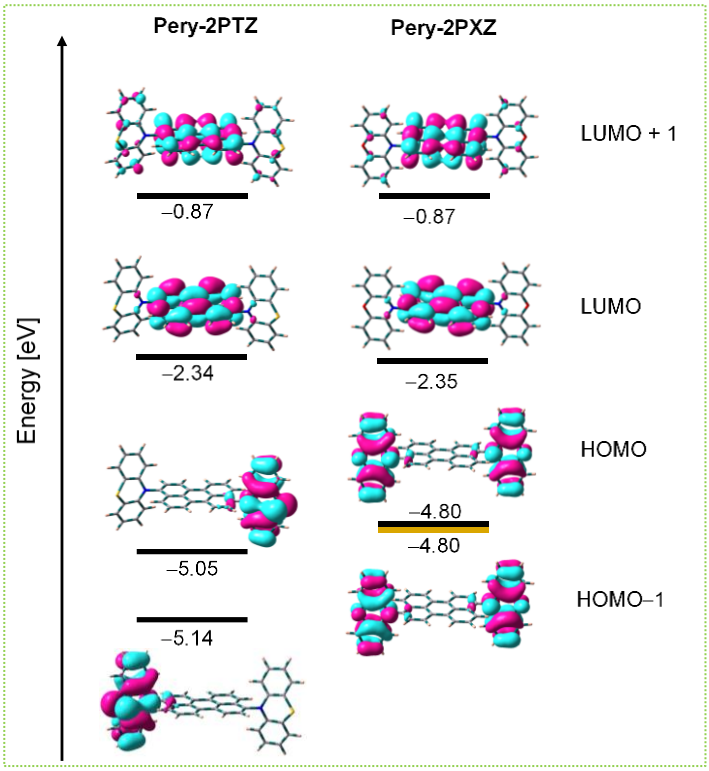

Fig. S36. Frontier molecular orbitals diagram of the triads at optimized singlet ground state geometries, using Gaussian 09 Level at B3LYP/6-31G.

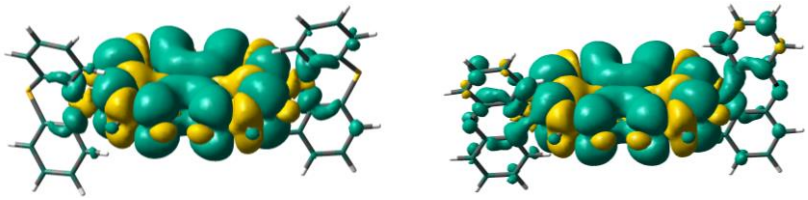

Pery-2PTZ **Pery-2PXZ**

Fig. S37. Isosurfaces of spin density distribution at optimized triplet state in ACN, using Gaussian 09 Level at B3LYP/6-31G.

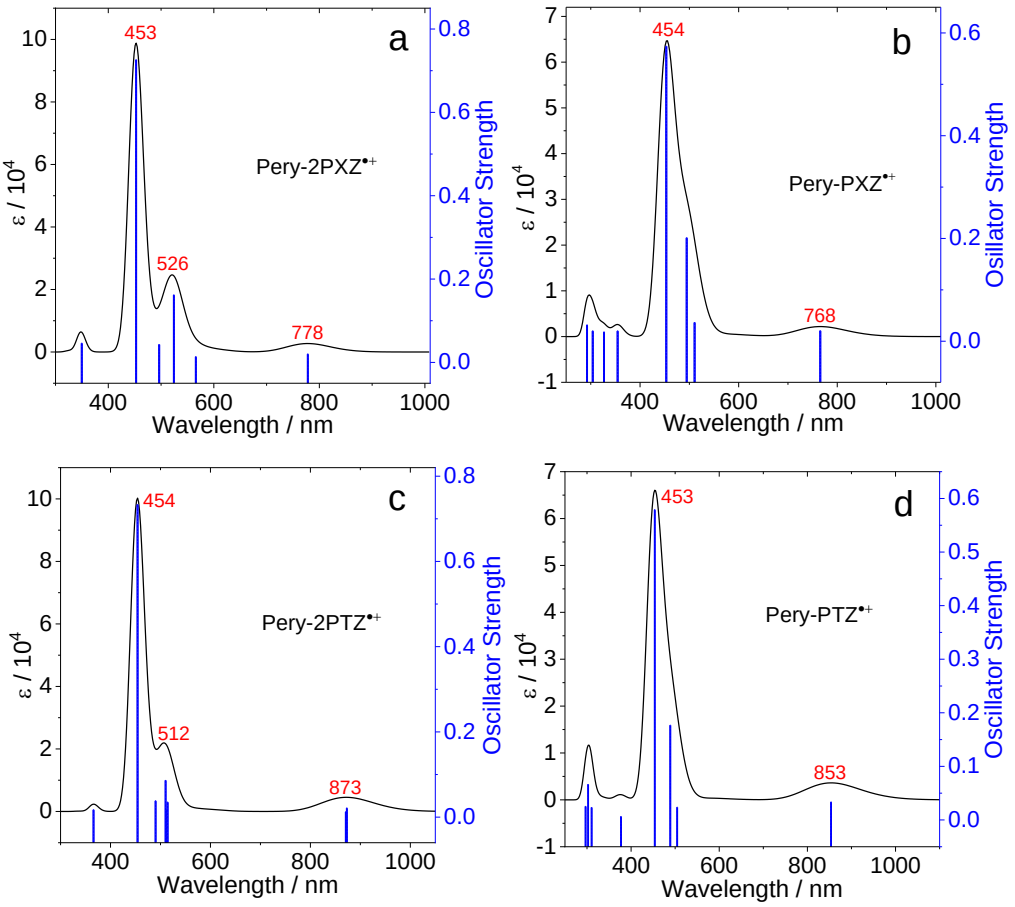

Fig. S38 DFT calculated UV−vis absorption spectra of (a) **Pery-2PXZ•+**, (b) **Pery-PXZ•+**, (c) **Pery-2PTZ•+** and (d) **Pery-PTZ•+**, in ACN (PCM model). Drop lines indicate oscillator strengths. The calculated spectra are obtained at the UB3LYP/6-31G(d) level using Gaussian 09.

Scheme S1. Simplified Jablonski diagram representing the photophysical processes involved in **Pery-2PXZ** upon direct photoexcitation[a]

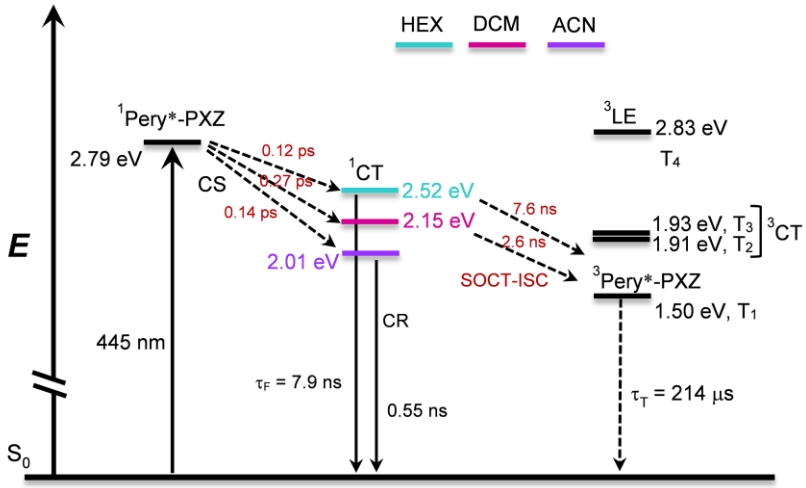

[a] The energy levels of the singlet excited states were derived from the spectroscopic data and the energy levels of the ^{1}CT states were obtained from the average of absorption and emission maxima and from the electrochemistry data. The energy levels of the triplet states were taken from TDDFT calculations. The numbers in superscript designate the spin multiplicity.

13. References

1. T. Matray. US Pat., WO 2017/197144 Al, 2017; Sony Corporation (Tokyo, JP), Sony Corporation of America (New York, NY, US).
2. K. Hayashi and M. Inouye, *Eur. J. Org. Chem.*, 2017, **2017**, 4334-4337.